Supplemental Data:

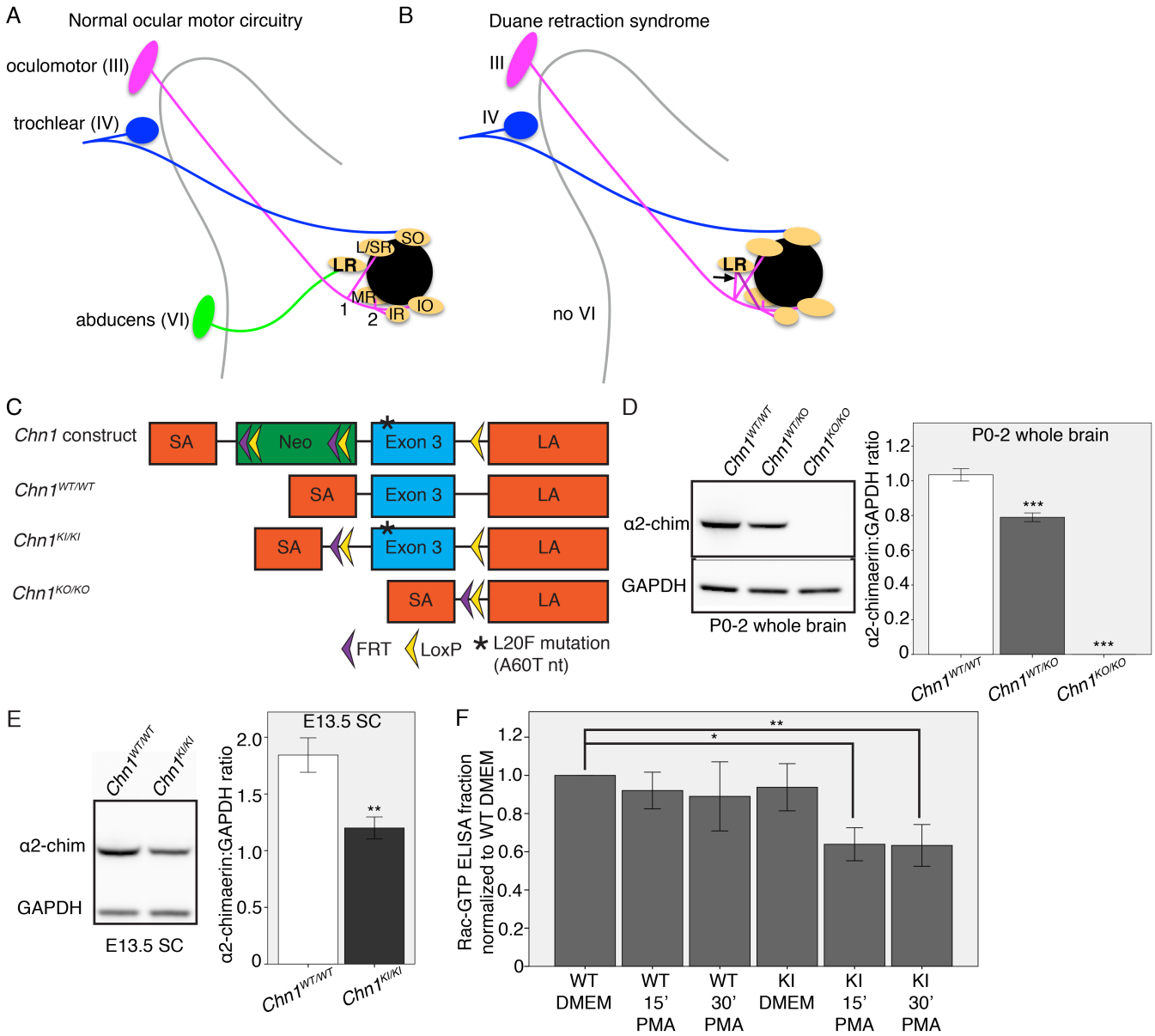

Supplemental Figure 1: *Chn1* knock-in and knockout mouse construct. (**A**) Normal ocular motor circuitry and innervation of extraocular muscles (EOM, beige) surrounding the eye (black). Abducens innervates lateral rectus (LR) muscle; oculomotor superior branch (1) innervates levator palpebrae superioris and superior rectus muscles (L/SR); oculomotor inferior branch (2) innervates medial rectus (MR), inferior rectus (IR), and inferior oblique (IO) muscles; trochlear innervates superior oblique (SO) muscle. (**B**) Ocular motor circuitry in Duane retraction syndrome. Abducens nucleus and nerve are absent; oculomotor nerve aberrantly innervates LR (arrow). (**C**) *Chn1* construct. Asterisk: 60A>T point mutation (L20F amino acid substitution) inserted into exon 3. Neomycin selection cassette (green) contains flanking FRT sites (purple chevron). LoxP sites (yellow chevron) flank Exon 3 to knock-out α2-chimaerin upon exposure to Cre-recombinase. LoxP sites flanking exon 3 preclude ability to cross $Chn1^{KI}$ line with Cre-expressing lines, instead causing conditional knockout of *Chn1*. (**D**) Western blot (left) and ratio quantification (right) of α2-chimaerin (top) and GAPDH (bottom) from P0-2 brain of littermate $Chn1^{WT/WT}$, $Chn1^{WT/KO}$, and $Chn1^{KO/KO}$ mice (n=3, *** p<0.001 by one-way ANOVA with Tukey's test). (**E**) Western blot (left) and ratio quantification (right) of α2-chimaerin (top) and GAPDH (bottom) from E13.5 spinal cord of $Chn1^{WT/WT}$ and $Chn1^{KI/KI}$ embryos (n=3 replicates from 8 pooled embryos, **p<0.01 by two-tailed t-test). (**F**) Rac-GTP ELISA of cultured cortical neurons from littermate E16.5-17.5 $Chn1^{WT/WT}$ (WT) and $Chn1^{KI/KI}$ (KI) mice, stimulated with DMEM (control), or PMA for 15 or 30 minutes (n=4; *p = 0.015, **p= 0.006 by unpaired two-tailed t-test, Bonferroni-corrected level of significance: p=0.016). Graphs represent mean ± SEM.

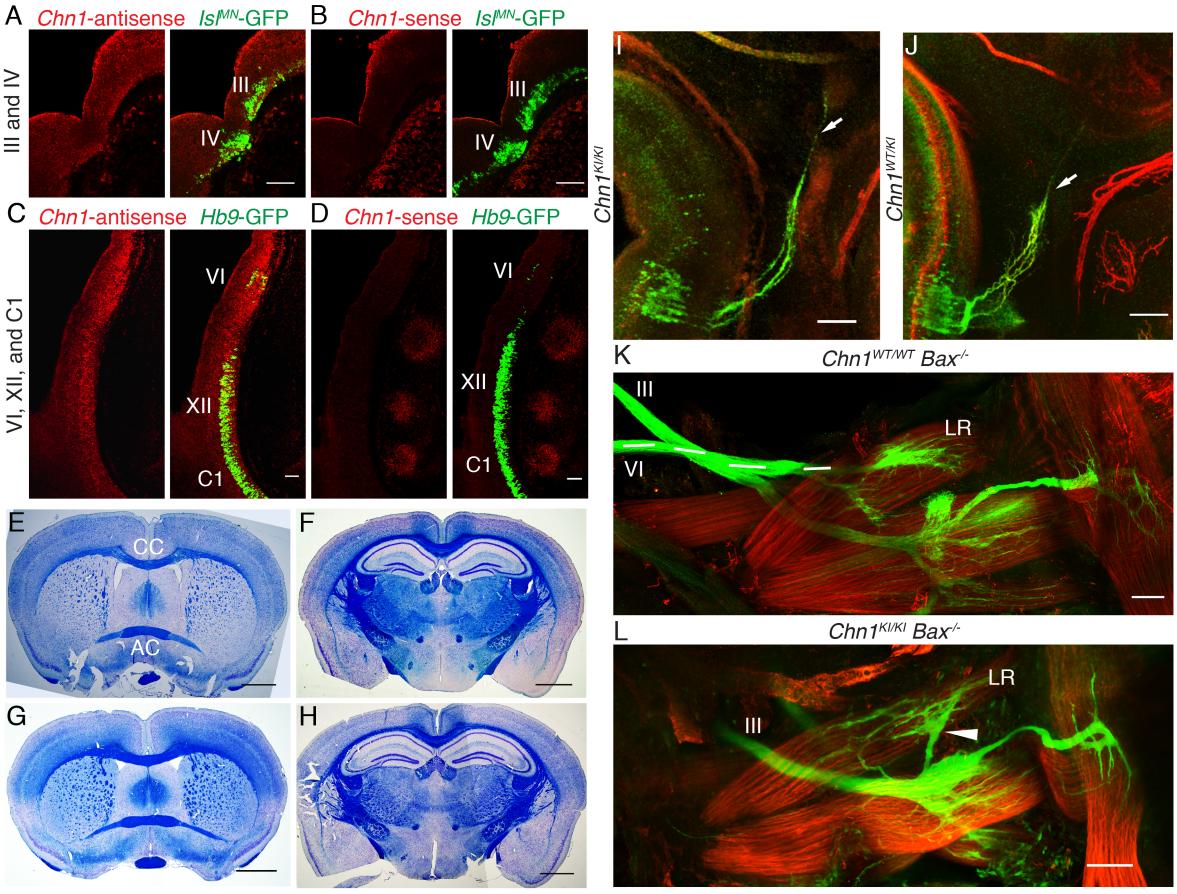

Supplemental Figure 2: *Chn1* expression, adult brain morphology, *Chn1*^{KI} embryonic abducens nerve phenotype spectrum, and *Chn1*$^{KI/KI}$ *Bax*$^{-/-}$ EOM innervation. (**A-B**) ISH for α2-chimaerin isoform of *Chn1* mRNA antisense (**A**) and sense (**B**) probes (red) with *GFP* antisense probe (green) on wildtype E11.5 sagittal section of oculomotor (III) and trochlear (IV) nuclei (*Isl*^{MN}-GFP). (**C-D**) ISH for α2-chimaerin isoform of *Chn1* mRNA antisense (**C**) and sense (**D**) probes (red) and *GFP* antisense probe (green) on wildtype E11.5 sagittal section of abducens nucleus (VI), hypoglossal nucleus (XII), and cervical spinal cord, including C1 (*Hb9*-GFP). (**E-H**) Luxol Fast Blue staining of coronal adult brain sections of *Chn1*$^{WT/WT}$ (**E, F**) and *Chn1*$^{KI/KI}$ (**G, H**) mice. N=3 mice for each genotype; CC: corpus callosum, AC: anterior commissure. (**I**) Thin *Chn1*$^{KI/KI}$ abducens nerve, arrow: remaining nerve bundle projecting to orbit. (**J**) *Chn1*$^{WT/KI}$ abducens nerve (n=5/10 nerves innervate from 5 embryos), arrow: stalling region. Red: neurofilament, green: *Hb9*-GFP. (**K-L**) Orbital innervation in E16.5 *Chn1*$^{WT/WT}$ *Bax*$^{-/-}$ (**K**; n=4 orbits) and *Chn1*$^{KI/KI}$ *Bax*$^{-/-}$ (**L**; n=6 orbits) embryos; white dashed line: abducens nerve (VI) trajectory; III: oculomotor nerve; arrowhead: oculomotor misinnervation of lateral rectus (LR). Red: actin α-smooth muscle, green: *Isl*^{MN}-GFP. Scale bars: 100μm (**A-D** and **I-L**), 1mm (**E-H**).

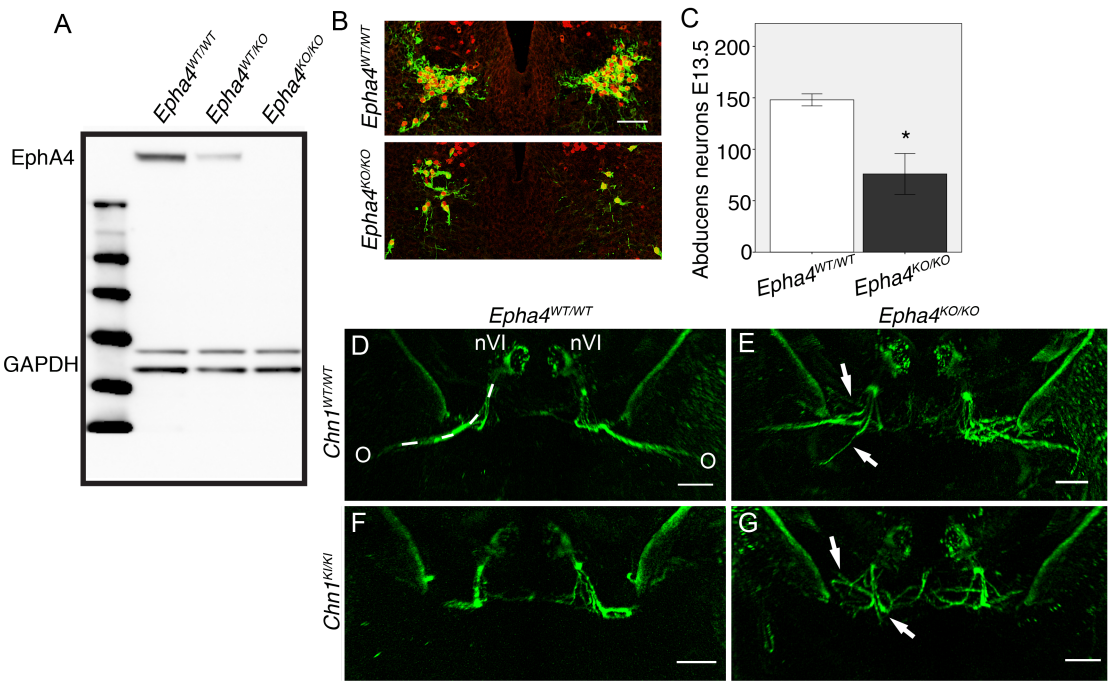

Supplemental Figure 3: *Epha4*$^{KO/KO}$ mice lack EphA4 protein; reduced abducens neuronal number in *Epha4*$^{KO/KO}$ embryos; raw transverse abducens nerve *Chn1*^{KI} *Epha4*^{KO} images. (**A**) Western blot of *Epha4*^{KO} *E2a*^{Cre} whole brain lysate from P0-P2 mice for EphA4 (top) and GAPDH control (bottom); n=3 brains for each genotype. (**B**) Representative images of *Hb9*-GFP abducens motor neurons at E13.5 in indicated genotypes; red: Isl1, green: *Hb9*-GFP; scale bar: 50µm. (**C**) Number of E13.5 abducens motor neurons for indicated genotypes. *Epha4*$^{WT/WT}$=3 embryos, *Epha4*$^{KO/KO}$=4 embryos; *p<0.05, unpaired t-test. (**D-G**) Raw images of transverse bilateral abducens nerve shown in Figure 5 from *Chn1*$^{WT/WT}$ *Epha4*$^{WT/WT}$ (**D**), *Chn1*$^{WT/WT}$ *Epha4*$^{KO/KO}$ (**E**), *Chn1*$^{KI/KI}$ *Epha4*$^{WT/WT}$ (**F**), and *Chn1*$^{KI/KI}$ *Epha4*$^{KO/KO}$ (**G**) E11.5 embryos. nIV: abducens nucleus; dashed white line: abducens nerve; O: orbit; arrows: wandering abducens nerve bundles; green: *Hb9*-GFP; scale bar: 100µm; n=4 embryos for each genotype.

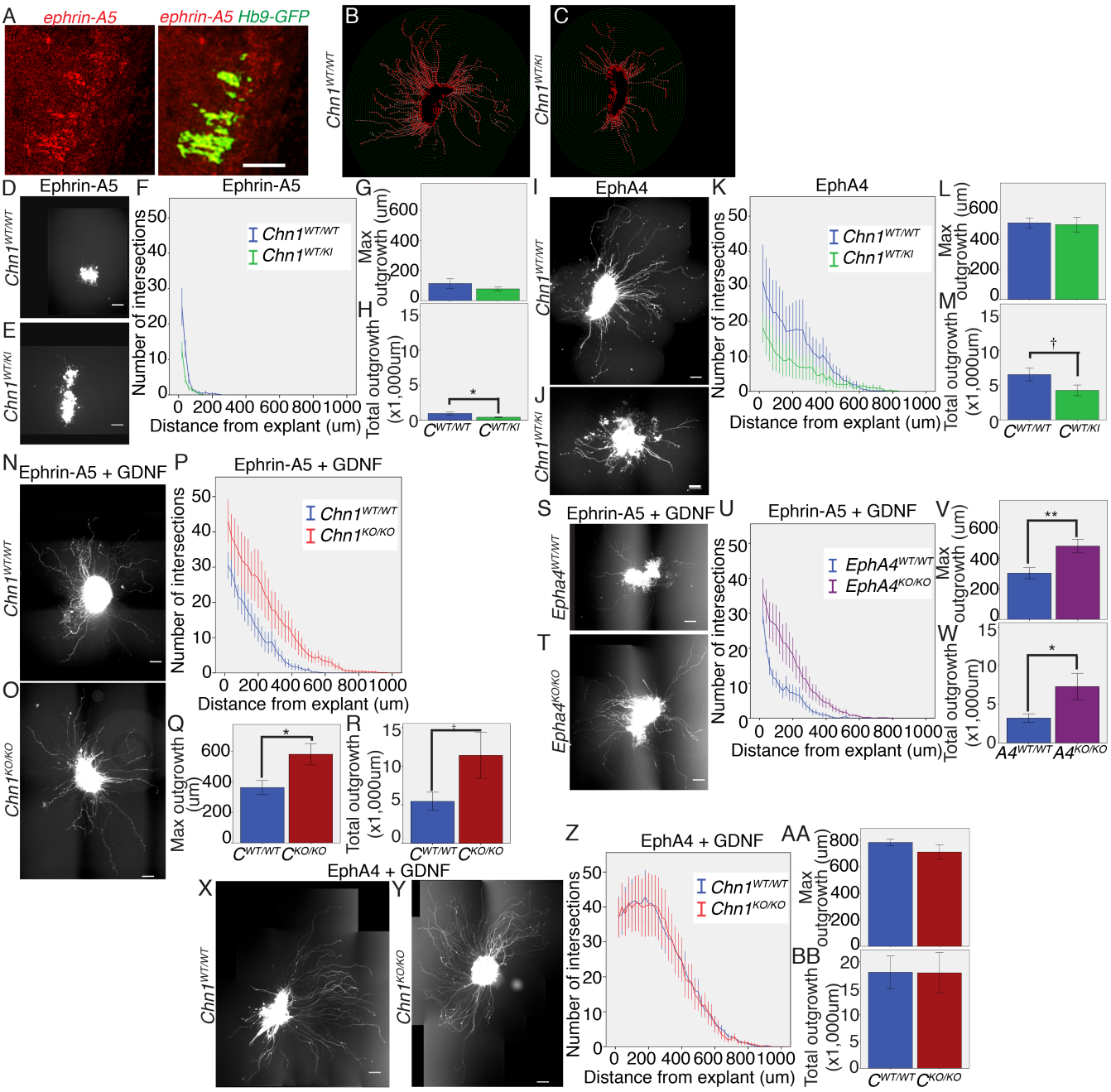

Supplemental Figure 4: *Chn1*$^{KO/KO}$ and *Epha4*$^{KO/KO}$ abducens explants similarly lack reduced outgrowth in ephrin-A5/GDNF. (**A**) *Ephrin-A5* (red) and *Hb9-GFP* (green) fluorescent ISH on sagittal section of E11.5 wildtype abducens nucleus; scale bar: 50μm. (**B-C**) Sholl images from *Chn1*$^{WT/WT}$ (**B**) and *Chn1*$^{WT/KI}$ (**C**) abducens explants grown in 1μg/mL EphA4 and 25ng/mL GDNF (from Figure 6, I-J). Red: abducens neurites, green: Sholl circles at 20μm intervals, white: counted intersections of Sholl circle with neurite.(**D-H**) Sholl analysis of *Chn1*$^{WT/WT}$ (**D**: n=7) and *Chn1*$^{WT/KI}$ (**E**: n=9) abducens explants grown in 50ng/mL ephrin-A5 (**F**: 3 experiments). (**G-H**) Quantification of maximum abducens outgrowth (**G**) and total outgrowth (**H**) from **F**. (**I-M**) Sholl analysis of *Chn1*$^{WT/WT}$ (**I**: n=32) and *Chn1*$^{WT/KI}$ (**J**: n=17) abducens explants grown in 1μg/mL EphA4 (**K**: 6 experiments). (**L-M**) Quantification of maximum abducens outgrowth (**L**) and total outgrowth (**M**) from **K**. (**N-R**) Sholl analysis of *Chn1*$^{WT/WT}$ (**N**: n=11) and *Chn1*$^{KO/KO}$ (**O**: red; n=10) abducens explants grown in 50ng/mL ephrin-A5 and 25ng/mL GDNF (**P**: 4 experiments). (**Q-R**) Quantification of maximum abducens outgrowth (**Q**) and total outgrowth (**R**) from **P**. (**S-W**) Sholl analysis of *Epha4*$^{WT/WT}$ (**S**: n=11) and *Epha4*$^{KO/KO}$ (**T**: purple; n=13) abducens explants grown in 50ng/mL ephrin-A5 and 25ng/mL GDNF (**U**: 3 experiments). (**V-W**) Quantification of maximum abducens outgrowth (**V**) and total outgrowth (**W**) from **U**. (**X-BB**) Sholl analysis of *Chn1*$^{WT/WT}$ (**X**: n=12) and *Chn1*$^{KO/KO}$ (**Y**: n=11) abducens explants grown in 1μg/mL EphA4 and 25ng/mL GDNF (**Z**: 3 experiments). (**AA-BB**) Quantification of maximum abducens outgrowth (**AA**) and total outgrowth (**BB**) from **Z**. † p<0.1, *p<0.05, **p<0.01, unpaired 2-tailed t-test. Graphs represent mean ± SEM. Scale bars: 100μm (**D-BB**).

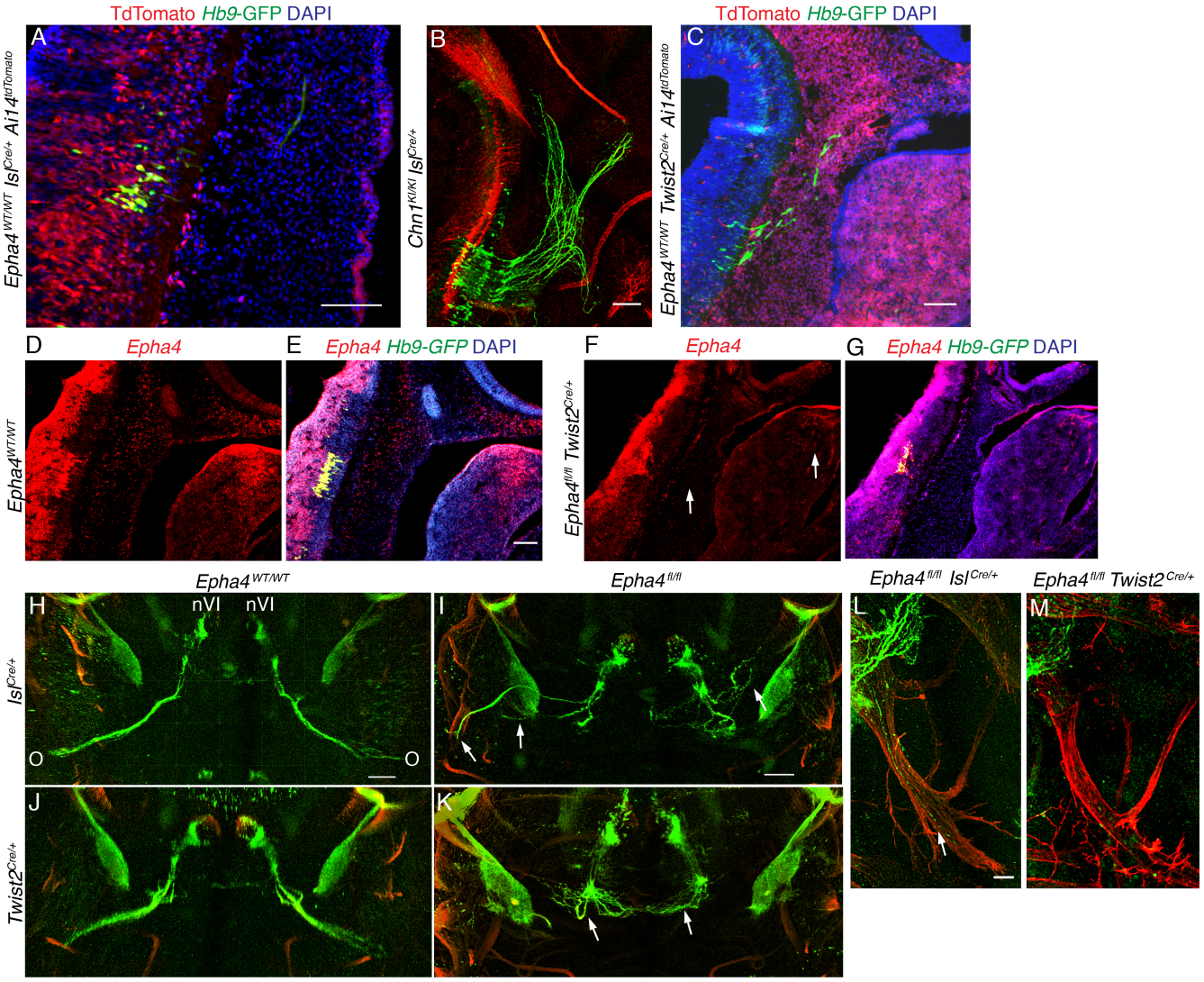

Supplemental Figure 5: *Isl*^{Cre} and *Twist2*^{Cre} expression; raw transverse abducens images. (**A**) Neuron-specific *Isl*^{Cre} expression in E11.5 *Epha4*$^{WT/WT}$ *Isl*$^{Cre/+}$ *Ai14*^{TdTomato} *Hb9*-GFP reporter embryo; red: TdTomato, green: *Hb9*-GFP. (**B**) *Chn1*$^{KO/KO}$-like abducens phenotype in *Chn1*$^{KI/KI}$ *Isl*$^{Cre/+}$ E11.5 embryo; n=3; red: neurofilament, green: *Hb9*-GFP. (**C**) Mesenchyme-specific *Twist2*^{Cre} expression in E11.5 *Epha4*$^{WT/WT}$ *Twist2*$^{Cre/+}$ *Ai14*^{TdTomato} *Hb9*-GFP reporter embryo; red: TdTomato, green: *Hb9*-GFP. (**D-G**) Wildtype (**D-E**) and *Epha4*$^{fl/fl}$ *Twist2*$^{Cre/+}$ (**F-G**) *Epha4* ISH (red) in *Hb9*-GFP^{+} embryos; green: *GFP*, blue: DAPI; arrows (**F**) indicate reduced *Epha4* in mesenchyme. (**H-K**) Raw images of transverse bilateral abducens nerve shown in Figure 8; nVI: abducens nucleus, O: orbit, arrows highlight wandering (**I**) and stalling (**K**) abducens projections; n≥3 embryos per genotype; red: neurofilament, green: *Hb9*-GFP. (**L-M**) Abducens fasciculation with mandibular and cervical facial nerve branches in E11.5 *Epha4*$^{fl/fl}$ *Isl*$^{Cre/+}$ (**L**) (arrow), but not *Epha4*$^{fl/fl}$ *Twist2*$^{Cre/+}$ (**M**) embryos; n≥3 embryos per genotype; red: neurofilament, green: *Hb9*-GFP. Scale bars: 100µm.

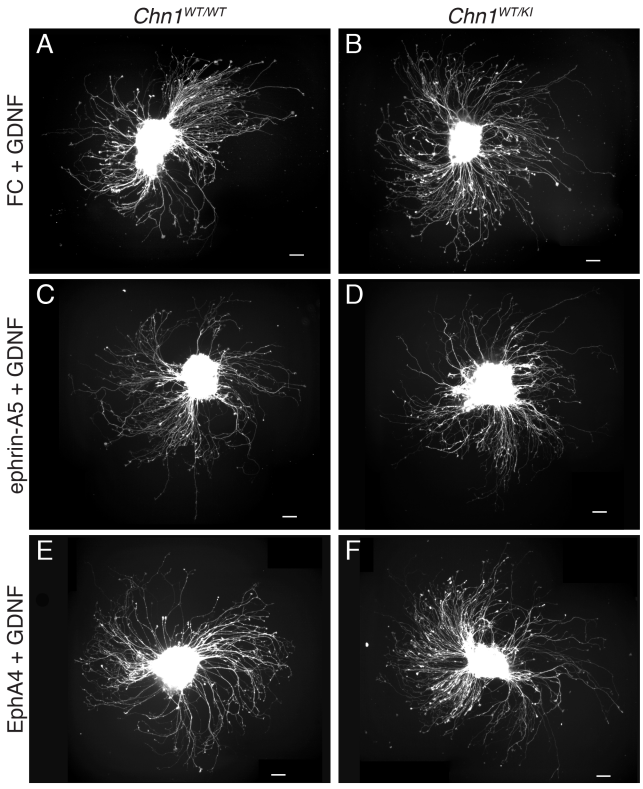

Supplemental Figure 6: *Chn1*^{KI} trochlear explants display minimal changes in outgrowth in response to ephrin forward and reverse signaling. (**A**-**F**) Images of E11.5 *Chn1*$^{WT/WT}$ (left) and *Chn1*$^{WT/KI}$ (right) *Isl*^{MN}-GFP-positive trochlear nucleus explants grown in 50ng/mL FC + 25ng/mL GDNF (**A-B**), 50ng/mL ephrinA5 + 25ng/mL GDNF (**C-D**), and 1µg/mL EphA4 + 25ng/mL GDNF (**E-F**). Scale bars: 100µm.

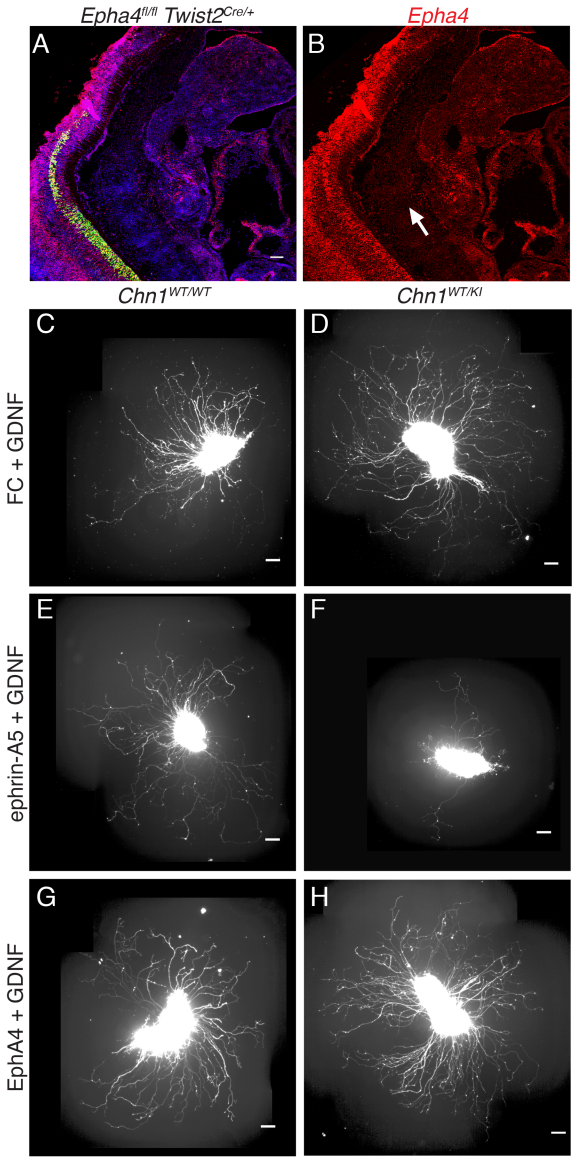

Supplemental Figure 7: *Chn1*^{KI} first cervical spinal segment (C1) explants show reduced outgrowth in response to ephrin forward signaling, but no outgrowth differences to ephrin reverse signaling. (**A-B**) *Epha4* expression remains in spinal cord of E11.5 *Epha4*$^{fl/fl}$ *Twist2*$^{Cre/+}$ embryo, but is reduced in mesenchyme (arrow); red: *Epha4*, green: *Hb9-GFP*, blue: DAPI. (**C-H**) Images of E11.5 *Chn1*$^{WT/WT}$ (left) and *Chn1*$^{WT/KI}$ (right) *Hb9*-GFP-positive C1 explants grown in 50ng/mL FC + 25ng/mL GDNF (**C-D**), 50ng/mL ephrinA5 + 25ng/mL GDNF (**E-F**), and 1µg/mL EphA4 + 25ng/mL GDNF (**G-H**). Scale bars: 100µm.

Supplemental Movies:

Supplemental Movie 1: *Chn1*$^{WT/WT}$ E11.5 whole mount embryo. For all whole mount embryo movies, red neurofilament staining highlights all developing cranial nerves and green marks endogenous *Hb9*-GFP, which is specifically expressed in VI, XII, and spinal motor neurons. Movie begins with a sagittal view, nose to the right and brainstem to the left. Abbreviations for all whole mount embryo movies: III: oculomotor, IV: trochlear, V: trigeminal, VI: abducens, VII: facial, XII: hypglossal, C1: first cervical spinal segment.

Supplemental Movie 2: *Chn1*$^{KI/KI}$ E11.5 whole mount embryo exhibits abducens nerve stalling, aberrant trochlear branching, and C1 misprojection. First arrow at 6 seconds: C1 misprojection; second arrow at 19 seconds: abducens stalling, third arrow at 33 seconds: multiple trochlear branches on the left side.

Supplemental Movie 3: *Chn1*$^{KO/KO}$ E11.5 whole mount embryo exhibits abducens nerve wandering. Arrow at 20 seconds: abducens misfasciculation with the buccal branch of the facial nerve. Trochlear and C1 nerves appear normal.

Supplemental Movie 4: Wildtype abducens growth cone collapse and axon retraction in response to bath application of ephrin-A5. First movie clip displays baseline abducens axon growth behavior across a 15 minute interval before application of ephrin-A5. Second movie clip displays growth cone collapse and axon retraction from the same abducens explant across a 30 minute interval after bath application of ephrin-A5.

Supplemental Movie 5: *Epha4*$^{KO/KO}$ E11.5 whole mount embryo exhibits abducens nerve wandering. First arrow at 12 seconds: abducens misfasciculation with the mandibular/cervical branch of the facial nerve; second arrow at 15 seconds: wandering abducens projection. Trochlear and C1 nerves appear normal.

Supplemental Movie 6: *Chn1*$^{WT/KI}$ *Epha4*$^{KO/KO}$ E11.5 whole mount embryo exhibits abducens nerve stalling and wandering, but restored C1 projection. First arrow at 4 seconds: rescued C1 projection; second arrow at 28 seconds: abducens misfasciculation with the mandibular/cervical branch of the facial nerve.

Supplemental Movie 7: *Epha4*$^{fl/fl}$ *Isl*$^{Cre/+}$ E11.5 whole mount embryo exhibits abducens nerve wandering. Arrow at 33 seconds: abducens misfasciculation with the mandibular/cervical branch of the facial nerve; note limited abducens projection to orbit. Trochlear and C1 nerves appear normal.

Supplemental Movie 8: *Epha4*$^{fl/fl}$ *Twist2*$^{Cre/+}$ E11.5 whole mount embryo exhibits abducens nerve stalling. Arrow at 13 seconds: abducens stalling and turning back toward hindbrain; note the abducens nerve does not reach the orbit.

Supplemental Methods:

Chn1^{KI} mouse construct. InGenious Targeting Laboratory, Inc. created the *Chn1^{KI}* targeting vector and inserted it into a mouse 129 (RP22:77N16) BAC clone. The 60A>T missense change (L20F amino acid substitution) was inserted into exon 3 of *Chn1* using two overlapping PCR fragments generated with forward primer PT5: GCTAGTCGCGAGTGTGTGAATTATGACATTTCTGC and mutation-containing reverse primer PT2: TGCTGCAGCTGGTA*A*ACTACAAGAAGGGAGAC (5' of exon 3 and extending to the point mutation), plus forward primer PT3: TGTCTCCCTTCTTGTAGT*T*TACCAGCTGCAGCAG and reverse primer PT6: GCTAGCTCGAGATTATGCTGTGACCCAGAG (from the point mutation to 3' of exon 3; point mutation in bold italics; added restriction sites are underlined: PT5 = NruI, PT6 = XhoI). The two primary PCR products were mixed and used as a template for a secondary PCR reaction, where PT5 and PT6 primers were used to amplify the entire sequence harboring the point mutation. NruI and XhoI were used to insert the PCR fragment into the wildtype BAC subclone. These restriction sites were engineered into the wildtype sequence using recombineering. The mutation-containing BAC was subcloned into a pSP72 ampicillin-resistant vector (Promega), then a pGK-gb2 loxP and FRT flanked neomycin selection cassette was inserted 5' to exon 3. A single loxP site was inserted 3' to exon 3. Presence of the mutation and proper insertion of the targeting vector were confirmed by restriction analysis and sequencing after each step. The mutation-containing BAC construct was injected into mouse embryonic stem (ES) cells by the Boston Children's Hospital IDDRC Mouse Gene Manipulation Core. Targeted ES cells were selected with the Neo cassette and screened using PCR, Southern blot, and sequencing for proper insertion and correct sequence. Additionally, knock-in mice were confirmed with genotyping primers Mut2F: GTAGGTGGAAATTCTAGCATCATCC and KIR: TGTGTGATGGGACTAAAGG. Subsequent offspring were crossed to *FLPe* mice (MGI: J:66893) to remove the Neo cassette.

Generation of Chn1^{KO} mice. Chn1$^{KI/KI}$ mice were crossed with *E2a-Cre* and *Prm-Cre* transgenic mice to create germline knockout *Chn1^{KO}* mice. Removing *Chn1* exon 3 preserves the promoter region and regulatory elements required for α1-chimaerin expression (40). Knockout was confirmed with genotyping PCR primers *Chn1* Common F: GGTTTTAAGCAGTCTCGGTGA and *Chn1* Common R: TCCGAATAAGCAATACAACCTTT and with α2-chimaerin Western blot on P0-2 whole brain lysate.

Additional mouse strains. Littermate controls were used whenever possible; controls from the same genetic background were always used for any given experiment. *Bax$^{-/-}$* (MGI: J:29253), *Epha4^{fl}* (MGI: J:157159), *Isl1^{Cre}* (MGI: J:107396), *Twist2^{Cre}* (MGI: J:81485), *Hb9*-GFP (MGI: J:88764), *Isl^{MN}*-GFP (MGI: J:132726), and *Ai14$^{ROSA26:tdTomato}$* (MGI: J:155793) mice are available from the Jackson Laboratory (Bar Harbor, ME), although at the time of initial experiments, *Isl^{MN}*-GFP mice were generously donated by Dr. Samuel L. Pfaff (Salk Institute for Biological Studies, La Jolla, CA). Mouse lines were

genotyped according to Jackson protocols. Notably, *Twist2* is located approximately 14MB from *Epha4* on chromosome 1. This caused linkage disequilibrium that required extensive breeding to obtain *Epha4*$^{fl/fl}$ *Twist2*$^{Cre/+}$ embryos (456 embryos to obtain 3 *Epha4*$^{fl/fl}$ *Twist2*$^{Cre/+}$ E11.5-E12 embryos).

Whole mount embryo staining. Chn1^{KI}, *Chn1*^{KO}, *Epha4*^{KO}, and *Epha4*$^{fl/fl}$ mice were crossed to *Hb9*-GFP mice. Resulting E11.5 embryos were fixed in 4% PFA and prepared as described previously (41). Whole embryos were stained with primary 1:500 mouse anti-neurofilament (clone 2H3, Developmental Studies Hybridoma Bank) and 1:500 rabbit anti-GFP (Invitrogen), then secondary 1:1000 goat anti-mouse Alexa Fluor 546 (Invitrogen) and 1:1000 goat anti-rabbit Alexa Fluor 488 or 647 (Invitrogen). Embryos were cleared with 1 part benzyl alcohol: 2 parts benzyl benzoate (Sigma; BABB), placed into a custom-designed, BABB-resistant holding chamber, and imaged using a Zeiss LSM710 laser scanning confocal microscope with Zen software (Zeiss). N≥3 embyros for all genotypes.

Whole mount image processing and analysis. Images were processed in 3D using Imaris (Bitplane) to identify similar z-planes between embryos. Sagittal images represent compressed z-stacks of 12µm step size and transverse images represent 8µm step compressed z-stacks. Compressed z-stack images from Imaris were uniformly processed in Fiji/ImageJ. Whole mount measurements were made in Fiji/ImageJ using the 546/neurofilament channel to enable measurements from GFP-positive and -negative embryos. Numbers of abducens nerve bundles were counted in the sagittal view, from the point at which neurofilament first appeared immediately after nerve bundles exited the hindbrain. Abducens nerve diameter was measured as previously described for oculomotor nerves (28). Briefly, diameter was measured in the sagittal view after fasciculation in Area 2 and before re-branching at the orbit region in Area 3 (Figure 1G). Abducens nerve length was measured in the sagittal view using Fiji Simple Neurite Tracer and accounted for x, y, and z-distances. Measurements were made from the hindbrain exit region, at the midpoint between the anterior and posterior nerve bundle exits, until the distal tip of the abducens nerve at the dorsal region of the orbit. Using the Imaris Surface tool, abducens nerves from transverse confocal images were processed to create a surface rendering of each nerve/nerve fiber. Images were manually compared to the raw image to ensure all visible abducens fibers were rendered in Surfaces. Resulting images were used to quantify the number of nerve fibers that deviated medially or laterally from the normal abducens nerve trajectory to obtain the wandering fiber measurement. Using the same transverse view, raw images were evaluated for trochlear nerve branching. The number of exited trochlear nerve branches on each individual side of the embryo was counted to obtain the trochlear branching measurement. Each experiment analyzed greater than three embryos from 3 or more independent litters.

Supplemental Table 1: Mouse strain information

Mouse line	Strain information
Chn1^{KI} Hb9-GFP	Mixed 129S1/6, C57BL/6J
Chn1^{KI} Isl^{MN}-GFP	Mixed 129S1/6, C57BL/6J, BALB/c
Chn1^{KO} Hb9-GFP	Mixed 129S1/6, C57BL/6J
Chn1^{KO} Isl^{MN}-GFP	Mixed 129S1/6, C57BL/6J, BALB/c
Chn1^{KI} Bax$^{-/-}$ Hb9-GFP	Mixed 129S1/6, C57BL/6J
Epha4^{KO} Hb9-GFP	Mixed 129S1/6/7, C57BL/6J, FVB/N, CD1
Epha4^{KO} Isl^{MN}-GFP	Mixed 129S1/6/7, C57BL/6J, FVB/N, CD1, BALB/c
Chn1^{KI} Epha4^{KO} Hb9-GFP	Mixed 129S1/6/7, C57BL/6J, FVB/N, CD1
Chn1^{KI} Epha4^{KO} Isl^{MN}-GFP	Mixed 129S1/6/7, C57BL/6J, FVB/N, CD1, BALB/c
Epha4^{fl} Isl^{Cre} Hb9-GFP	Mixed 129S1/6/7, C57BL/6J, FVB/N, CD1, Black Swiss
Epha4^{fl} Twist2^{Cre} Hb9-GFP	Mixed 129S1/6/7, C57BL/6J, FVB/N, CD1
Chn1^{KI} Isl^{Cre} Hb9-GFP	Mixed 129S1/6, C57BL/6J, Black Swiss

Western blot. Postnatal day 0-2 whole brain was homogenized on ice in RIPA buffer (Thermo Scientific), 1mM EDTA (Gibco), and Halt protease and phosphatase inhibitor cocktail (Thermo Scientific). E13.5 spinal cords were dissected and flash frozen in liquid nitrogen. After genotyping, 2-3 spinal cords from littermates of the same genotype were pooled and homogenized as above. Samples were incubated on ice for 30 minutes and clarified by spinning at 14,000rpm for 15 minutes at 4^0C. Supernatant protein concentration was measured using a BCA Protein Assay Kit (Pierce) on a NanoDrop 1000 (Thermo Scientific) and samples were adjusted to the same concentration within an experiment. After addition of NuPAGE LDS Sample Buffer (Invitrogen) and Sample Reducing Agent (Invitrogen), samples were incubated at 70^0C for 10 minutes. Denatured protein was run on a Western blot as described previously (28). Membranes were blocked with 5% milk in PBST, then incubated in 1:1000 rabbit anti-Chn1 (Abcam EPR9906), 1:500 rabbit anti-GAPDH (Santa Cruz), or 1:1000 mouse anti-EphA4 (BD Biosciences) overnight at 4^0C. Blots were washed 3X with PBST, then incubated in secondary antibody 1:5000 Peroxidase AffiniPure donkey anti-rabbit and/or donkey anti-mouse IgG (Jackson ImmunoResearch). Protein was detected using an Amersham ECL Prime Western Blotting Detection Reagent (GE Healthcare) and imaged with a FujiFilm LAS-4000 with CCD camera (GE Healthcare) and MultiGauge software (GE Healthcare). Experiments were performed with tissue from three different litters; n ≥ 3 samples per genotype.

Orbital dissections. E16.5 *Isl*^{MN}-GFP-positive mouse embryos from the indicated genetic crosses were fixed overnight in 4% PFA. Tissue around the orbit was removed, leaving the distal cranial nerves and EOMs intact. Orbits were incubated with 1:500 anti-actin α-smooth muscle-Cy3 antibody (Sigma-Aldrich) for 3 days at 4°C, washed 3X with PBS, then orbits were further dissected and flat mounted in 70% glycerol and 1% 1M KOH in PBS. Samples were imaged and processed as outlined for whole mount embryos. N $\geq$ 3 embryos from multiple litters were used for each genetic condition.

Chn1^{KI} *Bax*$^{-/-}$ *immunohistochemistry.* E10.5 and E13.5 *Chn1*^{KI} *Bax*$^{-/-}$ *Hb9*-GFP embryos were fixed overnight in 4% PFA, then dehydrated through a 25%, 50%, and 70% ethanol series. Embryos were embedded paracoronally in paraffin and serially sectioned at 10μm. Every fifth section underwent deparaffinization, and then placed in pre-boiled 1:100 Antigen Unmasking Solution (Vector Labs) in water and incubated for 20 minutes in a vegetable steamer. Sections were blocked with 1XPBS/0.3% TritonX100/5% heat-inactivated goat serum, stained overnight at 4^0C with 1:500 mouse anti-Isl1 (DSHB) and 1:500 chicken anti-GFP (Abcam), washed 3X PBS, incubated in secondary 1:1000 goat anti-mouse 546 (Invitrogen) and 1:500 goat anti-chicken FITC (Abcam) at room temperature for 1.5 hours, washed 3X PBS, stained with 1:1000 DAPI (Invitrogen), washed 2X PBS, and mounted in Fluoromount G (Southern Biotech). Sections were imaged using an Olympus BX51 fluorescence microscope. *Hb9*-GFP- and Isl1- positive abducens neurons were located anatomically, adjacent to *Hb9*-GFP-negative and Isl-positive facial neurons, then counted manually using ImageJ. Counts represent bilateral number of motor neurons. N $\geq$ 3 embryos from multiple litters were used for each age

and genetic condition and experiments were blinded.

Ephrin-A5 immunohistochemistry: E11.5 *Hb9*-GFP embryos were fixed in 4% PFA overnight at 4^0C. Embryos were incubated for 12 hours in 20% Sucrose/PBS, then 12 additional hours in 30% Sucrose/PBS before embedding for sagittal sectioning in O.C.T. (TissueTek). Samples were cryosectioned at 20µm. Sections were blocked in 5% Goat Serum/0.3% TritonX-100/PBS, and stained with 1:50 rabbit anti-ephrin-A5 (R&D Systems), then 1:1000 goat anti-mouse Alexa Fluor 546, then mounted and imaged as above. N≥3 slides were analyzed from 2-3 wildtype embryos.

In situ hybridization (ISH): E11.5 embryos were prepared and embedded as described above. Digoxigenin (DIG)-labeled mRNA antisense probes to α2-chimaerin specific *Chn1, Epha4, ephrin-A5*, and *EGFP* were generated using the noted primers: *Chn1-F* GTAACTTTTCCTCGCTGCGG, *Chn1-R* GTGCTGTTTGTATGCTGGCT*; Epha4_exon15-F* CAGTTAATGCTGGACTGCTGGC, *Epha4_ exon15-R* GACCTCATTTGTCCAGTTAGGG; *Epha4_exon3-F* TGCGAACTGACTGGATCACC *Epha4_exon3-R* TTGACACAGGAGCCTCGAAC*; ephrin-A5-F* CCCTCAGCCCCAGTTGGTCA, *ephrin-A5-R* CAGCCCCACTGAGCCTTCCT; and a fluorescein (FITC)-labeled probe against *EGFP* was made using plasmid DNA of the full length sequence of *EGFP* (pEGFP-C1) as a template. ISH on 20µm sections was performed by the RNA In Situ Hybridization Core at Baylor College of Medicine using an automated robotic platform as previously described (42) with modifications for double ISH. Modifications in brief: both probes were hybridized to the tissue simultaneously (*Chn1/EGFP*, *ephrin-A5/EGFP*, or *Epha4/EGFP*). After the described washes and blocking steps, the DIG-labeled probes were visualized using tyramide-Cy3 Plus (1/50 dilution, 15 minute incubation, Perkin Elmer). After washes in TNT, the remaining HRP-activity was blocked by a 10 minute incubation in 0.2M HCl. The tissue was then washed in TNT, blocked in TNB for 15 minutes before a 30 minute room temperature incubation with HRP-labled sheep anti-FITC antibody (1/500 in TNB, Roche). After washes in TNT the FITC-labeled probe was visualized using tyramide-FITC Plus (1/50 dilution, 15 minute incubation, Perkin Elmer). Following washes in TNT the slides were stained with DAPI, washed again, removed from the machine and mounted in ProLong Diamond (Molecular Probes). N=3 slides were analyzed for each probe from 1-3 wildtype embryos.

Rac-GTP ELISA: 12 well plates were coated with 50µg/mL poly-D-lysine. E16.5-17.5 mice were decapitated, then the brain was carefully removed and placed in ice-cold PBS. Genotyping was performed during dissections and dissociation. Each cortical hemisphere was microdissected in HBSS, avoiding lateral aspects. Both cortical hemispheres were cut into small pieces and placed into an individual eppendorf tube. Tissue was dissociated in Papain according to manufacturer instructions (Worthington, Inc.) and resuspended in Neurobasal medium as outlined above. Cells from the same genotype within a litter were combined into one sample and cultured for 40-48 hours at $1x10^6$ cells/mL. Experiments were always conducted simultaneously with wildtype and

mutant littermates. Cells were serum starved in DMEM/Penicillin/Streptomycin for 2 hours, then DMEM or 10μM PMA in DMEM was added (DMEM: 30 minutes, PMA: 15 or 30 minutes). Cells were washed 1X with cold PBS, then lysed in ice cold RIPA buffer with 1mM EDTA and 1X protease and phosphatase inhibitor (as outlined for Western blot). Samples were immediately spun at 14000g for 10 minutes at 4^0C and supernatant was stored at -80^0C. Samples were processed for Rac-GTP levels using a Rac1 G-LISA Activation (Colorimetric Based) Assay Kit (Cytoskeleton, Inc.) as recommended by the company's protocols. When possible, two replicates per condition were run on the same plate and O.D. output values were averaged. Averaged values were normalized to the O.D. values obtained from wildtype DMEM within each experiment. N=4 experiments from 4 litters.

Abducens, trochlear, and C1 explant culture. Acid washed and autoclaved German glass coverslips (VWR) were placed into 24-well plates and coated with 20μg/mL poly D-lysine (Millipore) in PBS overnight at 37^0C. Wells were washed 3X with water, then coated with 10μg/mL laminin (Invitrogen) in PBS for 2 hours at 37^0C. *GFP*-positive embryos were harvested in ice cold PBS and microdissected in ice cold HBSS. Abducens explants: The hindbrain was carefully separated from *Hb9*-GFP-positive embryos using fine forceps and dissected along the dorsal surface in an open-book manner to reveal the abducens nuclei. Meningeal tissue was removed from the ventral hindbrain. GFP-negative tissue surrounding each individual abducens nucleus was carefully trimmed away with a tungsten needle, leaving two intact explants per embryo. Both nuclei were placed into PDL/laminin coated wells with HBSS on ice during dissection of the remaining littermates. Trochlear explants: Isl^{MN}-GFP-positive midbrain tissue was dissected as outlined above. Trochlear nuclei were distinguished from oculomotor by their caudal anatomical location, carefully dissected from GFP-negative tissue, and placed into PDL/laminin coated wells with HBSS on ice. C1 explants: C1 was identified anatomically in *Hb9*-GFP-positive embryos and removed with rostral and caudal cuts flanking the cervical segment. Dissection proceeded as outlined above. Due to the larger size of C1, dissected explants were divided into 2 equally sized pieces for each embryonic side using a tungsten needle, yielding 4 explants per embryo. 2 explants from the same unilateral side were placed in PDL/laminin-coated wells containing HBSS on ice. For each well, the two explants were positioned at opposite sides of the coverslip, HBSS was removed, and quickly replaced with Neurobasal (Invitrogen), 1X B27 (Invitrogen), 2mM L-glutamine (Invitrogen), and 100μg/mL Penicillin/Streptomycin (Invitrogen) containing indicated growth factors and/or proteins. Explants were cultured at 37^0C in a cell culture incubator (5% CO_2/95% air).

Growth cone collapse experiments. Abducens explants were grown in 25ng/mL GDNF, 25ng/mL BDNF, and 25ng/mL CNTF for 12-14 hours, then transferred to a Nikon Perfect Focus Eclipse Ti live cell fluorescence microscope using Elements software (Nikon), where they were maintained at 37^0C in an environmental chamber with 5% CO_2/95% air. Explants were imaged once a minute for 15 minutes to assess initial growth cone dynamics. 100ul of media was removed, indicated recombinant proteins

were added, and the mixture was applied. Explants were reimaged every 60 seconds for 30 minutes to assess growth cone dynamics with noted cues. Collapsed growth cones were quantified as any growth cone with fewer than 3 filopodia and no lamellipodia. Axon retraction was quantified as any axon that regressed more than the distance equal to one growth cone. For each condition, n≥95 axons from ≥3 independent experiments.

Sholl analysis. Abducens, trochlear, and C1 explants were grown in noted growth factors and proteins for 18 hours, then fixed for 1 hour at room temperature with 4% PFA and 4% sucrose in PBS. Explants were imaged on the Nikon Eclipse Ti fluorescence microscope. Images from each explant were tiled into a single image using a Fiji macro developed by the Harvard NeuroDiscovery Core. A second Fiji macro subtracted background fluorescence, applied a standard threshold to individual images (abducens and C1: triangle dark, trochlear: mean dark), and saved images as a mask. The explant body was outlined manually in Fiji then a final macro drew concentric circles at 20µm intervals and counted intersecting axons. The number of intersecting axons per 20µm interval was exported to Excel. N ≥ 11 explants were used from 3 or more independent experiments. Wildtype controls were present in each replicate within every condition (i.e. ephrinA5+GDNF), and different protein combinations (i.e. ephrinA5+GDNF and FC+GDNF) were compared within at least one experiment per group. Using SPSS, individual samples were graphed within each condition to assess distribution, and then averaged across experiments within each condition to obtain final outgrowth curves. To assess initial outgrowth, intersections between 0-200µm were summed and multiplied by 20µm to yield an initial outgrowth integral value, then averaged across samples of a given condition. Averaging the micron distance of the last intersecting circle across all samples of a given condition generated the maximum outgrowth value. To assess total outgrowth, intersections for each individual sample across all distances were summed and multiplied by 20µm to yield a total outgrowth integral value, then averaged across samples of a given condition.

Additional Funding Information. The project described was supported in part by the RNA In Situ Hybridization Core facility at Baylor College of Medicine, which is supported by a Shared Instrumentation grant from the NIH (1S10OD016167) and the NIH IDDRC grant U54HD083092 from the Eunice Kennedy Shriver National Institute Of Child Health & Human Development. The content is solely the responsibility of the authors and does not necessarily represent the official views of the Eunice Kennedy Shriver National Institute Of Child Health & Human Development or the National Institutes of Health.